Applied Geochemistry 88 (2018) 103–112

Contents lists available at ScienceDirect

Applied Geochemistry

journal homepage: www.elsevier.com/locate/apgeochem

Application of surface complexation modeling to trace metals uptake by biochar-amended agricultural soils

Md. Samrat Alam [a], Logan Swaren [a], Konstantin von Gunten [a], Manuel Cossio [a], Brendan Bishop [a], Leslie J. Robbins [a], Deyi Hou [b], Shannon L. Flynn [a, 1], Yong Sik Ok [c, d], Kurt O. Konhauser [a], Daniel S. Alessi [a, *]

[a] Department of Earth and Atmospheric Sciences, University of Alberta, Edmonton, AB T6G 2E3, Canada
[b] Division of Groundwater and Soil Environment, School of Environment, Tsinghua University, Beijing 100084, China
[c] Korea Biochar Research Center, Kangwon National University, Chuncheon 24341, Republic of Korea
[d] O-Jeong Eco-Resilience Institute (OJERI), Division of Environmental Science and Ecological Engineering, Korea University, Seoul, Republic of Korea

ARTICLE INFO

Article history:
Received 28 February 2017
Received in revised form
18 July 2017
Accepted 20 August 2017
Available online 24 August 2017

ABSTRACT

Biochar has emerged as a useful amendment to release nutrients into agricultural soil, to increase crop productivity, and as a sorbent to remediate metals and organics contamination. Since soils have heterogeneous physical properties across a given crop field, and even over a growing season, it is imperative to select the most appropriate biochar for the intended purpose and in defining the amendment level. In this study, we investigate the adsorption of Cd(II) and Se(VI) as model pollutant cations and anions, respectively, to two agricultural soils amended with a wood pin chip biochar (WPC). The proton reactivity of each sorbent was determined by potentiometric titration, and single-metal, single-sorbent experiments were conducted as a function of pH. The resulting data were modeled using a non-electrostatic surface complexation modeling (SCM) approach to determine the proton and metal binding constants and surface functional group concentrations of each soil and WPC. The SCM approach is a considerable advance over empirical modeling approaches because SCM models can account for changes in pH, ionic strength, temperature, and metal-to-sorbent ratio that may happen over the course of a growing season. The constants derived from the single-metal, single-sorbent experiments were then used to predict the extent of metal adsorption in more complex mixtures of Cd, Se, soil and WPC. Overall the SCM approach was successful in predicting metal distribution in multi-component mixtures. In cases where the predictions were poorer than expected, we identify reasons and discuss future experiments needed to further the application of SCM to sorbent mixtures containing biochar.

1. Introduction

Biochar is an increasingly popular soil amendment used to enhance or modify natural microbial activity (e.g., Anders et al., 2013; Masiello et al., 2013; Kappler et al., 2014; Zhang et al., 2014), to release nutrients critical for crop growth (e.g., Uchimiya et al., 2010; Laird and Rogovska, 2015; Lehmann et al., 2015), and as a remediation technique to immobilize contaminants in soil and water (e.g., Rees et al., 2014; Ahmad et al., 2014; Alam et al., 2016). In part because biochar shows promise in contributing to global carbon sequestration (Woolf et al., 2010), research on its properties and uses has expanded dramatically in the past decade (Verheijen et al., 2014). Understanding how biochar amendment impacts the distribution of trace metals, and ultimately their transport in soils, is critical to its ongoing use in agricultural applications. Römkens et al. (2002) and Bonten et al. (2008), using agricultural soils in the Netherlands as an example, point out that metal leaching is an underappreciated and understudied contributor to the metals loads of surface waters. Furthermore, soil and water geochemistry in crop fields are not static; considerable temporal and spatial variations in pH, nutrient and metals phytoavailability occur (Andersson and Bingefors, 1985; Cambardella et al., 1994; López-Granados et al., 2002; Zhao et al., 2011). In this context, a flexible approach to

* Corresponding author.
E-mail address: alessi@ualberta.ca (D.S. Alessi).
[1] Present address: School of Natural and Environmental Sciences, Newcastle University, Newcastle upon Tyne, United Kingdom.

http://dx.doi.org/10.1016/j.apgeochem.2017.08.003
0883-2927/

predicting the impacts of biochar amendment on metal mobility in agricultural soils is required.

Most of the current literature on metals adsorption to biochar-amended soil, and indeed on biochar and soils themselves, employs empirical adsorption models, such as the linear distribution coefficient (K_D) and various adsorption isotherms (e.g., Freundlich, Temkin, Langmuir) to fit data from adsorption experiments. While useful at the conditions under which the experiments are conducted, predictions of metal distribution from these models are often not valid if parameters such as pH, solution ionic strength, sorbate-to-sorbent ratios, and temperature change in the system of interest (Bethke and Brady, 2000; Koretsky, 2000). In addition, the models do not consider the aqueous speciation of metals or the underlying mechanisms of metal adsorption. By contrast, surface complexation models (SCMs) offer an alternative, and more mechanistic approach. SCMs use a system of equations approach to consider the chemical speciation of solutes, the type and concentration of discrete reactive surface sites on sorbents in the system, and the formation of surface complexes with defined stoichiometries. For equations in the system, which represent individual chemical reactions, a mass action constant (K) is defined which describes conditions at which the reactants and products are at equilibrium, because K satisfies conditions for which the Gibbs free energy of reaction ($\Delta_r G$) is nil (Garrels and Christ, 1965; Anderson, 2005). These systems of equations can then be solved to predict the equilibrium distribution of sorbates of interest in the system over a wide range of pH, ionic strength, and sorbate-to-sorbent ratios, and can also consider the competition of multiple sorbates for binding to discrete sites on the sorbent surfaces.

As SCMs consider numerous molecular-scale reactions, they are inherently more complex and data-intensive than empirical adsorption modeling approaches. As Goldberg (1992) notes, SCMs of soil-metal interactions often use only a few types of surface sites, while in reality soils are always far more complex and contain numerous types of sites. In fact, describing the protonation and metal adsorption behavior of individual soil components themselves, such as bacteria (e.g., Fein et al., 1997; Cox et al., 1999; Fein, 2006; Alessi et al., 2010), metal oxides (e.g., Davis et al., 1978; Dzombak and Morel, 1990; Lalonde et al., 2007a; Komárek et al., 2015), carbonates (Lalonde et al., 2007b; Flynn et al., 2017) organic matter (e.g., Smith and Kramer, 1999; Petrash et al., 2011), and clays (e.g., Schroth and Sposito, 1997; Kraepiel et al., 1999; Lund et al., 2008), typically requires invoking more than one binding site. Because of this complexity, Davis et al. (1998) proposed two methods to model metal distribution in complex assemblages of sorbents using the SCM approach: the component additivity (CA) approach and the general composite (GC) approach. The CA approach is premised on first developing protonation and metal adsorption models for each major sorbent in the complex assemblage, which yields binding site densities, pK_a values, and mass action constants for metal binding for each sorbent. Predictions about the equilibrium metal distribution in admixtures of the sorbents can then be made by invoking combinations of the models developed for each sorbent at the ratios in which those sorbents are present in the admixture being considered.

However, there are some limitations to the CA approach. For example, it is well known that organic ligands can both complex metals in solution and lead to the formation of ternary metal-ligand-surface complexes on sorbents (Davis, 1984). In an application of the CA approach, Alessi and Fein (2010) successfully described Cd(II) adsorption to admixtures of kaolinite, planktonic *Bacillus subtilis* cells, and hydrous ferric oxide (HFO). When a model organic ligand, acetate (CH_3COOH), was added to the system, it became necessary to invoke the adsorption of $Cd(CH_3COO)^+$ to sorbent surface sites to explain the observed Cd(II) adsorption behavior. Additionally, blockage of reactive sites may occur when sorbents aggregate in mixtures; for example, this was noted by Zachara et al. (1992) who reported that HFO may block fixed-charge sites on kaolinite, thereby inhibiting Cd(II) adsorption. Kulczycki et al. (2005) observed similar impacts of site blockage when modeling the adsorption of Pb(II) and Cd(II) to admixtures of HFO and bacteria. Thus, the formation of ternary complexes and sorbent site blockage are two potential limitations that should be considered when applying the CA approach.

The general composite (GC) approach uses a single protonation model to describe complex, multi-component sorbents. In the case of a soil, generic functional groups - derived from the modeling of potentiometric titration data - are assigned to describe the protonation behavior of the whole soil. Assigning these generic sites allows for the flexibility and predictive ability inherent in the SCM approach, but without specific knowledge of the identity of those surface sites. Davis et al. (1998) used the GC approach to overcome difficulties in modeling Zn(II) adsorption to complex mineral assemblages.

While the application of SCMs to soils and their components is well-studied, research that applies surface complexation theory to model metal adsorption to biochar is now just emerging. Zhang and Luo (2014) successfully modeled Cu(II) adsorption to a biochar produced from an anaerobic digester sludge, and Vithanage et al. (2015) developed a two-site electrostatic SCM to describe the adsorption of antimony (Sb) to a soybean-stover biochar. Despite this recent progress, to the knowledge of the authors, no multi-sorbent surface complexation model that includes biochar has been developed. Accordingly, in this paper, we investigated the impact of biochar amendment on Cd(II) and Se(VI) adsorption to two agricultural soils collected from a canola (*Brassica rapa*) and an alfalfa (*Medicago sativa*) field in Alberta, Canada. While Cd and Se are contaminants of concern in agricultural soils and to human health (Holmgren et al., 1993; Tan et al., 2002; Grant and Sheppard, 2008; Banuelos et al., 2013), these metals are used in this study primarily as a model cation and anion, respectively, in order to test the SCM approach on biochar-soil mixtures. A non-electrostatic SCM was developed for Cd and Se adsorption to the biochar and each of the two whole soils. Using these models, the CA approach is then used to predict the distribution of Cd and/or Se in mixtures of one of the soils and the biochar. Where the CA approach does not predict Se or Cd adsorption well, we discuss reasons for those disparities, and more broadly identify ongoing challenges in applying the SCM approach to sorbent mixtures that contain biochar.

2. Materials and methods

2.1. Soil and biochar collection and preparation

Two agricultural soils were collected in September 2016, approximately 60 km NNW of Edmonton, Alberta, Canada from a canola field (54° 5′ 26″ N 113° 52′ 29″ W) and an alfalfa field (54° 2′ 45″ N 113° 59′ 60″ W), hereafter referred to as CFS and AFS, respectively. The CFS was a solonetzic to solonetz soil, moderately well drained, with a 15–25 cm thick A horizon and a 15–25 cm thick B horizon; the AFS was a luvisolic soil, well drained, with a 15–30 cm thick A horizon and a 10–20 cm thick B horizon (Kjeargsgaard, 1972). To collect soil samples representative of each field, sampling locations were selected to be away from the entrances/exits and close to the center of the fields. The topsoil was removed with a shovel to a depth of five to eight centimeters below the surface with another shovel that was cleaned before sampling. Sampling went as deep as 20 cm below surface (12–15 cm below the bottom of the topsoil) and approximately 5 kg of soil was

obtained from both the canola and alfalfa fields. Plastic bags containing the soils were sealed and transported to the University of Alberta. Once samples were dried, sieves were used to separate soil fractions. The soil fraction smaller than 1 mm was used for potentiometric titrations and metal adsorption experiments.

A wood pin chip biochar (WPC) from the Alberta Biochar Initiative (ABI) was produced by the pyrolysis of wood pin chip feedstock in a batch carbonizer under oxygen-limited conditions. Temperature in the pyrolysis unit was raised from 20 °C to 500 °C over a period of 60 min, and then held between 500 °C and 550 °C for 30 min. The resulting WPC was sieved to 2 mm prior to use in titration and metal adsorption experiments. The pH of each material was determined by suspending 0.5 g of solids in 50 mL of water, and placing the mixture on a rotary shaker for 24 h prior to measuring pH (Novak et al., 2009).

2.2. Materials characterization

2.2.1. Elemental composition

Total metal composition of soil and biochar samples was determined by digestion with hydrofluoric acid (HF). Prior to the described digestion, the biochar was ashed at 500 °C over 8 h to digest the material (von Gunten et al., 2017). For this purpose, 0.1 g of the dried soil sample was pretreated with 5 mL 70% nitric acid (HNO_3, ACS grade, Fisher Scientific) and 5 mL 30% hydrogen peroxide (H_2O_2, ACS grade, Fisher Scientific) and left to react for 1 h. The sample was then heated on a hot plate at 130 °C for 3 h. 5 mL HF (47–51%, ACS grade, Fisher Scientific) was added to each vessel and evaporated at 130 °C, before 3 mL 37% hydrochloric acid (HCl, ACS grade, Fisher Scientific) and 1 mL HNO_3 were added to dissolve the remaining residue. The solution was heated to near dryness at 130 °C, and finally diluted to 50 mL with 2% HNO_3 and 0.5% HCl. Aqua regia extractable metals were determined for the soil samples to account for possible Se losses through evaporation. This was done by adding 6 mL HCl (37%) and 2 mL HNO_3 (70%) to 0.1 g of dried soil material. The solution was heated to near dryness at 130 °C on a hot plate, and finally diluted to 50 mL with 2% HNO_3 and 0.5% HCl. The reference material STSD-3 (CANMET Mining and Mineral Sciences Laboratories) was digested in parallel to verify elemental recovery. Metals and metalloids were analyzed using inductively coupled plasma mass spectrometry operated with two mass separating quadrupoles (ICP-MS/MS; Agilent 8800) and using a reaction cell with collision gases according the manufacturer's instruction. Sample analyses were conducted in triplicate, and Indium (500 ppb) was used for internal calibration. The contents of C, H, O, and N in the soils and biochar were measured by combustion at 1000 °C using an elemental analyzer (Carlo Erba EA1108). Dry combusted total organic carbon (TOC) and water extracted dissolved organic carbon (DOC) of AFS, CFS, and WPC were determined using a TOC analyzer (Shimadzu TOC-V/TN).

2.2.2. Sequential extractions for metals

The two soils were characterized by sequential extraction according to a modified method by Tessier et al. (1979) and Li et al. (1995) to determine the elemental composition and distribution of elements in various sediment fractions. Extractions were performed on untreated, fresh samples and samples to which metals were sorbed. A more detailed account of the sequential extraction method is provided in the supplementary information.

2.2.3. Powder X-ray diffraction, clay content, pedogenic oxides and cation exchange capacity (CEC)

Powder X-ray diffraction (XRD) was conducted on each of the soils and WPC to identify major crystalline phases in the materials. Prior to analysis, the materials were ground to a fine powder using a mortar and pestle, and analyzed using an X-ray diffractometer (Rikagu Ultima IV) with a cobalt source, between a 2θ range of 5°–90°. Resulting diffraction patterns were fit using the JADE 9.5 analysis package (KS Analytical Systems).

The clay fraction in the soils, defined as less than 2 μm, was determined using particle size analyses (PSA) using the hydrometer method, and laser PSA using the Fraunhofer optical model. Major and minor oxides were calculated based on the total digestion data. Loss of ignition (LOI) was calculated from the elemental analysis data (see Table 1). Cation exchange capacity (CEC) of AFS, CFS, and WPC was determined as described in Robertson et al. (1999).

2.2.4. Scanning electron microscopy

Materials were imaged using a scanning electron microscope (SEM; Zeiss EVO LS15) equipped with an energy dispersive X-ray spectroscopy (EDS) system (Bruker Quantax 200) for semi-quantitative measurement of elemental composition. Prior to analysis, samples were carbon coated using an evaporative carbon coater (Leica EM SCD005). Secondary electron images were captured using an Everhart-Thornley detector, and backscatter electrons were collected with a Si-diode detector.

2.3. Titration and metal adsorption experiments

2.3.1. Potentiometric titrations

Potentiometric titrations of each soil sample and biochar were conducted to determine their proton buffering capacities. To prepare for titration, the pH electrode (Metrohm 905 Titrando) was calibrated using a set of three pH buffers, and then placed in a covered sample cup containing a magnetic stir bar, dispensers for acid (0.1 M HCl) and base (0.1 M NaOH) titrants, and 50 mL of electrolyte solution (0.01 M $NaNO_3$) containing 0.2 g of soil or biochar. The solution was bubbled for 30 min prior to the start of a titration, and continuously for the duration of the titration with N_2 gas, to prevent the introduction of atmospheric $CO_2(g)$ into the solution. Titrations were conducted by initially adding acid to bring the solution to pH 3, then a forward (base) titration to pH 10, and finally a reverse titration to pH 3. Forward and reverse titrations were preformed to monitor for irreversible alterations to the soils and biochar which could result in hysteresis. All titrations were performed in dynamic addition mode whereby the titrator adds a variable volume acid or base (0.5 μL–0.15 mL) depending on the buffering capacity observed during the previous addition. New additions were only made after the pH electrode achieved a stability 0.2 mV s^{-1}. A blank titration of just the background electrolyte solution (0.01 M $NaNO_3$) was performed to quantify its proton buffering capacity, which was subtracted from the titrations of each

Table 1
Physical properties of alfalfa field soil (AFS), canola field soil (CFS), and wood pin chip biochar (WPC).

Properties	Sample		
	AFS	CFS	WPC
pH	5.30	5.00	9.70
%C	2.90	2.05	84.60
%H	0.70	0.50	2.10
%O	4.90	3.36	9.40
%N	0.25	0.20	0.20
Molar H/C	2.80	3.00	0.30
Molar O/C	1.25	1.22	0.08
TOC (w/w%)	2.90	2.26	82.11
DOC (mg/L)	14.04	23.84	105.90
Clay fraction (<2.0 μM) in volume (%)	19.16	18.37	NA
Clay fraction (<3.806 M) in volume (%)	28.79	27.72	NA

NA = not available.

of the materials.

Non-electrostatic surface complexation models were developed for AFS, CFS, and WPC. To solve for proton binding constants (pK_a) and site concentrations for each material, we fit the potentiometric titration data for each material using the least-squares optimization software FITEQL 4.0 (Herbelin and Westall, 1999). In the models, the deprotonation of a discrete number of surface functional groups is represented by the equilibrium reaction:

$$>R-A_i-H^0 \leftrightarrow >R-A_i^- + H^+ \quad (1)$$

where $>R$ represents the soil or biochar particle to which proton-active surface functional group A_i is attached. The associated mass action equation for reaction (1) is defined as:

$$K_a = \frac{\left[>R-A_i^-\right] a_{H^+}}{\left[>R-A_i-H^0\right]} \quad (2)$$

where K_a is the protonation constant, a_{H^+} represents the activity of protons in solution, and terms in brackets represent the molal concentrations of protonated and deprotonated surface functional groups.

To fit the titration data for each material, between one to four ($i = 1-4$) discrete sites were tested. FITEQL solves simultaneously for the functional group concentration and pK_a for each site. Best fit was determined by: (a) whether model convergence was achieved, and (b) the value of the variance parameter, V(Y), calculated in FITEQL; values of $1 \leq V(Y) \leq 20$ are generally considered to be a good fit (Westall, 1982).

2.3.2. Metal adsorption experiments

Batch metal adsorption experiments were conducted with Se(VI) and Cd(II). To initiate an experiment, the soils were suspended to a concentration of 10 g L^{-1} or the biochar to 1 g L^{-1} in a solution containing either 0.1 mM Cd(II) as $Cd(NO_3)_2$, or 0.1 mM Se(VI) as Na_2SeO_4. While being agitated with a stir bar, 10 mL aliquots of a suspension were transferred to a set of twelve 15 mL polypropylene test tubes. Individual test tubes in the set were adjusted with small volumes of concentrated acid or base to cover a pH range between approximately 2 and 8. Higher pH was avoided to prevent Cd(II) precipitation as solid carbonate or hydroxide species (Liu et al., 2015; SI Fig. 1). Tubes were sealed and placed on an end-over-end rotator. As needed, the pH of tubes was adjusted with acid or base to maintain the target pH. The experiments were allowed to equilibrate for 12 h after the final pH adjustment, after which they were centrifuged at 10,000 g for 10 min (Sorvall Lynx 4000). The resulting supernatants were filtered through 0.45 μm nylon membranes, acidified with 5 μL of 10 M HNO_3, and stored in the dark at 4 °C until analysis. Concentrations of Cd and Se were measured using an ICP-MS/MS (Agilent 8800) with an in-line internal standard addition system. Cd was analyzed using no-gas mode (i.e., no additional gas was introduced to the reaction chamber). Se was analyzed in two different modes: in no-gas mode, and by introducing 10% O_2 gas into the reaction chamber to apply a mass shift of 16. The resulting pH adsorption edge data were used to calculate the binding constants of Cd(II) and Se(VI) to each soil and the biochar.

Multi-sorbent and multi-metal experiments were conducted according to the protocol outlined above. In multi-sorbent experiments, 10 g L^{-1} of a soil was mixed with 1 g L^{-1} biochar, and either 0.1 mM Cd(II) or 0.1 M Se(VI). Multi-metal experiments included 10 g L^{-1} of a soil or 1 g L^{-1} of biochar, added to a mixture of 0.1 mM Cd(II) and 0.1 mM Se(VI). Finally, dual-metal/dual-sorbent experiments were conducted by combining 10 g L^{-1} soil, 1 g L^{-1} biochar, 0.1 mM Cd(II), and 0.1 mM Se(VI). An additional set of experiments containing 5 g L^{-1} soil, 5 g L^{-1} biochar, and 0.1 mM each of Cd(II) and Se(VI) were conducted to further test the predictive capability of the SCM CA approach. For all data sets, binding constants calculated from the single-metal, single-sorbent systems, described above, were used to predict the extent of metal adsorption in the multi-component systems.

Using the protonation models developed for each sorbent (Section 2.3.1), metal binding constants were calculated. Cd(II) adsorption to the sorbent surface functional groups defined in the protonation models is described by:

$$>R-A_i^- + Cd^{2+} \leftrightarrow >R-A_i-Cd^+ \quad (3)$$

and the corresponding Cd binding constant, $K_{i\text{-}Cd}$, is defined by:

$$K_{i-Cd} = \frac{\left[R-A_i-Cd^+\right]}{\left[R-A_i^-\right] a_{Cd^{2+}}} \quad (4)$$

where $a_{Cd^{2+}}$ represents the activity of the Cd^{2+} species in aqueous solution, and $[R-A_i-Cd^+]$ is the molal concentration of the Cd-surface complex formed at functional group A_i of a sorbent.

Selenate adsorption is best described by invoking two types of surface complexes, following reactions described in Goldberg (2014) as follows:

$$>R-O-H^0 + HSeO_4^- + H^+ \leftrightarrow >R-HSeO_4^0 + H_2O \quad (5)$$

$$>R-O-H^0 + HSeO_4^- \leftrightarrow >R-SeO_4^- + H_2O \quad (6)$$

With Se(VI) surface complexation mass action constants defined for reactions (5) and (6) as:

$$K_{1-Se} = \frac{\left[>R-HSeO_4^0\right]}{\left[>R-O-H^0\right] a_{HSeO_4^-} a_{H^+}} \quad (7)$$

$$K_{2-Se} = \frac{\left[>R-O-SeO_4^-\right]}{\left[>R-O-H^0\right] a_{HSeO_4^-}} \quad (8)$$

respectively. The models then invoke outer-sphere complexation of Se at site 1 of the sorbents (equations (5) and (7)), and inner-sphere Se complexation at site 2 (equations (6) and (8)). The major Cd(II), Se(VI) and carbonate aqueous species were considered in the models (SI Table 1).

3. Results and discussion

3.1. Soil and biochar physical properties

The complete results of the HF digestion for AFS, CFS, and WPC are listed in SI Table 2, and presented for selected major elements in Fig. 1. The average elemental recovery for the standard STSD-3 for the HF digestion and the sequential extraction (sum) were 99% and 81%, respectively, suggesting some elemental losses through the extraction procedure. The soil metal compositions of AFS and CFS are qualitatively similar. The major mineral phases found in both soils include quartz, albite, and phyllosilicates such as kaolinite, muscovite, and clinochlore (SI Fig. 2). The pedogenic oxides calculation also supports the interpretation of a dominant quartz fraction in the two soils (SI Table 3). Silicate-rich soils are further characterized by the high concentrations of Si measured during SEM-EDS analyses (SI Figs. 3 and 4). Only the Mn concentration was

notably different, with AFS containing approximately 33% more than CFS. WPC biochar contained relatively lower concentrations of Mg, Al, Ca, and Fe than the soils. Quartz was the only mineral phase identified by XRD (SI Fig. 2). In all cases the digestion of soils with aqua-regia released less metals than the digestion with HF (Fig. 1); no Se or Cd was measured in the soils or biochar (SI Tables 1, 3, 4). Despite the similarities in metals and mineral content, AFS contains considerably more C, H, N, and O, and a higher soil pH, than CFS (Table 1).

Sequential extraction results for unaltered AFS, CFS, and WPC samples are shown in Fig. 1. In the soils, phosphorus was mainly found in the residual fraction (74%–80% of the total), suggesting the presence of highly insoluble phosphate-bearing solids. In the soils, S was dominant in the organic matter fraction (62%–71%), indicating the presence of sulfide phases, while in WPC, S was found in the exchangeable and residual fractions (39% and 33% of the sum, respectively). The total digestion of biochar suggests an even larger residual fraction with up to 84% S. Calcium was primarily found in the exchangeable fractions of the soils (67%–71% of the sum) and in the carbonate fraction of WPC (39% of the sum). Most of the Ca in all materials was not released by aqua regia extraction, indicating that more resilient Ca-containing phases are present. Potassium and Fe were bound mostly to the residual fraction of soils, dominantly in silicate minerals. The contribution of the (amorphous) Fe/Mn-oxide

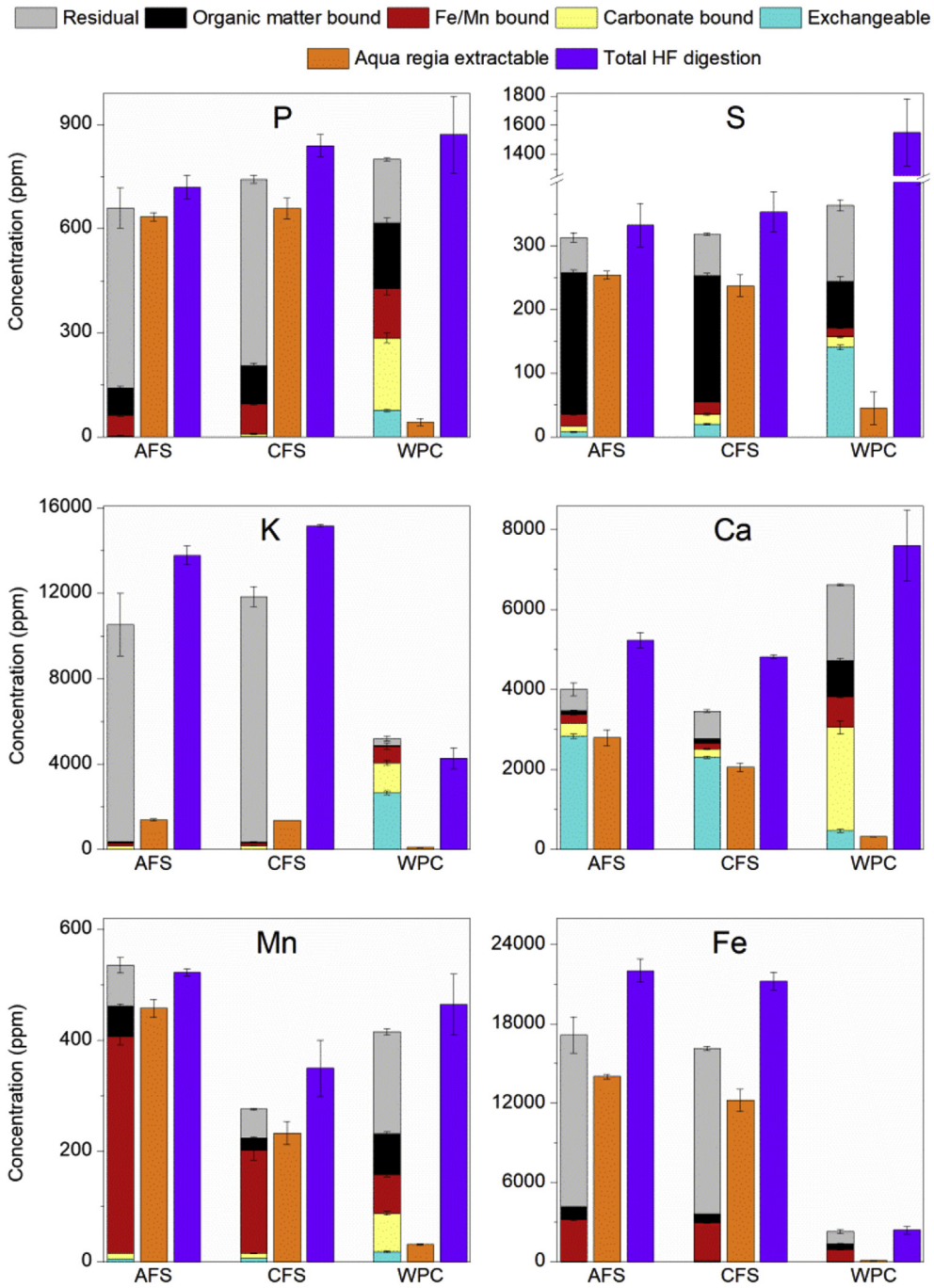

Fig. 1. Sequential extraction results for the soils AFS and CFS and the biochar WPC. The values are shown together with aqua regia extractable metals and HF digestion results. Error bars represent standard deviation (n = 3) at a 95% confidence interval.

fraction for Fe was very small in the soils (18%), but greater in WPC (41%). This was in stark contrast to Mn, with a Fe/Mn-oxide fraction of 63%–73% of the total value in the soils, and 17% in WPC. These results imply the presence of amorphous Mn phases in soils and Fe phases in biochar. Trace metals, such as Ni, Zn, and Pb, were dominant in the residual fractions of the untreated samples (SI Fig. 5). On average, only 11% of those metals were bound to Fe/Mn-oxides, while approximately 9% were found in the organic matter fraction.

Sequential extractions were repeated after Cd(II) and Se(VI) were sorbed to the soils and WPC. After the sorption experiments, Cd was dominantly found in the exchangeable fractions of soils and biochar (Fig. 2). At pH 3, no other fraction contributed substantially to Cd sorption. At pH 7, more Cd was adsorbed, and the exchangeable fractions contained on average 81% of all Cd. In all three samples, only a minor fraction of Cd uptake was associated with the carbonate and the amorphous Fe/Mn extraction fractions. Thus, Cd is likely bound to the samples by cation exchange and adsorption to amorphous Mn oxides and clay minerals (soils) and Fe oxides (biochar).

Selenium was mostly found in the organic matter/sulfide fraction of the soils at both pH levels tested (Fig. 2). On average, 58% of Se in soils was in this fraction, in contrast to the biochar at pH 7, where approximately 6% of Se was found in the organic matter/sulfide fraction and 86% was in the exchangeable fraction. We can conclude that the uptake of Se is dominated by organic particles and sulfides in the soils under acidic and neutral pH conditions. At neutral pH conditions, WPC contributes considerably to Se uptake, but it is only weakly bound to the material matrix. The cation exchange capacity (CEC) of WPC is high as compared to the soils (SI Table 5). The NH_4-N extraction method revealed that Ca exchange is highest in both the soils and the biochar, followed by Mg in the soils and by K in WPC. The exchange of Fe, Mn, and Al is negligible in both soils and the biochar.

3.2. Protonation models of the sorbents

For all three materials, a two-site model provided the best fit for the potentiometric titration data (Table 2; SI Fig. 6). The pK_a values for AFS and CFS were similar (2.3 and 6.5 for AFS; 2.4 and 7.0 for CFS), which is consistent with their similar mineralogy and composition. The pK_a values for WPC, 4.3 and 7.5, were considerably different than those of the soils.

3.3. Single metal adsorption experiments

Single metal adsorption experiments to each sorbent showed the expected increase in Cd(II) adsorption with increasing pH, and decreasing Se(VI) adsorption with increasing pH (Fig. 3). AFS adsorbs both Cd and Se somewhat stronger than CFS, perhaps due to a somewhat higher organic content (Table 1) and higher concentration of proton-active functional groups (Table 2). Generally, the Cd and Se metal binding constants to the two surface functional groups used to describe the soils are similar, while binding constants for WPC differ from the two soils (Table 3). By invoking Cd adsorption to the two binding sites determined in the protonation models, we fit the Cd experimental adsorption data for all three sorbents (Fig. 3a; SI Fig. 7). However, we were unable to explain Se adsorption to AFS or CFS by invoking any combination of inner- and/or outer-sphere Se complexation to the two binding sites. Operationally, this was due to the nearly linear decline in Se(VI) adsorption between pH 2 and 8, an unusual pH edge shape that suggests that another Se(VI) reaction should be considered. The presence of dissolved organic carbon (DOC) may explain the observed discrepancy, either by its forming complexes with Se(VI) that keep it in dissolved form, or by promoting the formation of Se(VI)-DOC-surface ternary complexes. For example, Bolan et al. (2003) observed that DOC derived from soils formed soluble complexes with Cu, and Beesley et al. (2015) noted the co-mobilization of DOC and metals in soils amended with biochar. To test whether DOC in solution contributed significant proton-active functional groups to the solutions in soil metal adsorption experiments, we allowed AFS and CFS to equilibrate with the solution for 24 h, and then conducted potentiometric titrations of the supernatants after filtration through 0.45 μm nylon membranes. The DOC titration data were fit with a 1-site non-electrostatic SCM, using the methods described in Section 3.2. DOC in solution contributed considerable buffering capacity, comparable to the soils themselves, and the low pK_a values calculated (Table 3) were consistent with those of soil DOC, which are known to be low (e.g., Nambu and Yonebayashi, 1999). These DOC protonation models were used to solve for the formation of an inner-sphere Se-DOC complex, according to Equation (6) above. Invoking a solution Se-DOC complex resulted in acceptable Se fits to AFS and CFS adsorption data (Fig. 3b; SI Fig. 8).

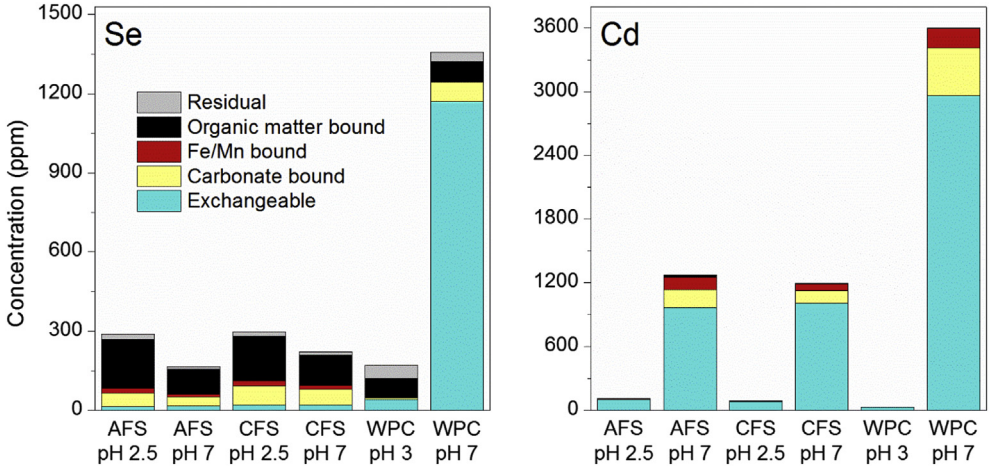

Fig. 2. Sequential extraction results from soils and biochar to which Se and Cd had been pre-sorbed at pH 2.5 and pH 7 (soils) and pH 3 and pH 7 (biochar).

Table 2
Best-fit pKa and site concentrations for each sorbent, and the supernatants leached from AFS and CFS soils at pH 7, following equilibration.

Materials	Sites	pKa_1	pKa_2	Site 1 concentration (mol/g)	Site 2 concentration (mol/g)	V(Y)
WPC	2	4.3	7.5	1.03E-03	1.93E-04	13
AFS	2	2.3	6.5	8.58E-04	3.01E-04	15
CFS	2	2.4	7.0	8.43E-04	2.41E-04	23
AFS DOC	1	2.7		1.32E-03		10
CFS DOC	1	1.5		1.26E-04		1

Table 3
Best-fit metal binding constants (K) for Cd(II) and Se(VI) adsorption to AFS, CFS, and WPC.

Samples	Sites	log K_{Cd1}	log K_{Cd2}	V(Y)	log K_{Se1}	log K_{Se2}	log K_{DOCSe}	V(Y)
AFS	2	0.31	−0.90	6	−0.60	7.40	9.70	17
CFS	2	0.16	−1.38	6	−0.50	7.40	5.40	6
WPC	2	−2.34	−3.62	26	−1.85	7.92		37

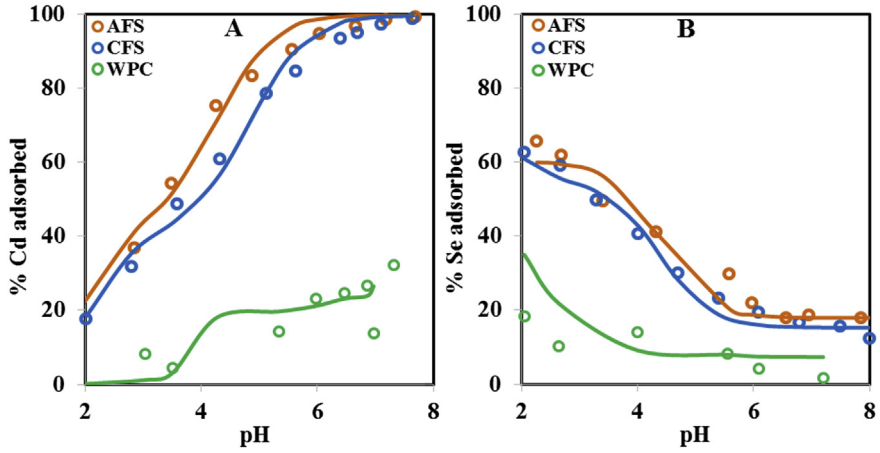

Fig. 3. Adsorption of (A) 100 μM Cd and (B) 100 μM Se, to AFS (10 g L^{-1}), CFS (10 g L^{-1}), and WPC (1 g L^{-1}). Open symbols represent experimental data and solid lines represent best-fit surface complexation modeling fits.

3.4. Multi-component adsorption experiments and model predictions

To test the non-electrostatic SCMs developed in Sections 3.2 and 3.3, sorbents and sorbates were mixed in various combinations. The pK_a values, site concentrations, and metal binding constants calculated from the single-metal, single-sorbent experiments were used to predict the extent of metal removal from solution in the more complex systems. Fig. 4 illustrates the adsorption of Cd(II) (panel A) and Se(VI) (panel B) to mixtures containing one of the soils and WPC, thus simulating a biochar-amended agricultural soil. The addition of 1 g L^{-1} WPC to 10 g L^{-1} of soil did not greatly increase the extent of metal removal from solution as compared to the soils-only experiments (Fig. 3). In all four cases tested, model predictions were a close match to the experimental data (Fig. 4). Similarly, model predictions were excellent for systems containing one sorbent and two metals (0.1 mM Cd(II) and 0.1 mM Se(VI); Fig. 5), and the adsorption behavior of each metal was again similar to that of the single-metal, single-sorbent experiments (Fig. 3). This indicates that Cd and Se were not competing measurably for binding onto surface functional groups of AFS, CFS, or WPC.

Two-sorbent, two-metal experiments were conducted at two sorbent ratios to fully test the predictive capability of the SCM. At 10 g L^{-1} soil and 1 g L^{-1} WPC, the extent of Cd and Se adsorption was predicted with reasonable accuracy from pH 2 to 8 (Fig. 6). Further experiments were conducted at sorbent concentrations of 5 g L^{-1} soil and 5 g L^{-1} biochar. Clearly an agricultural soil will not be amended with 50% (w/w) biochar, and so this was an experimental exercise to further test the SCM CA approach under more extreme conditions. The model yielded acceptable predictions of Cd(II) adsorption, but poor predictions of Se(VI) removal from solution (Fig. 7). There are several potential explanations. Firstly, only modest Se(VI) removal is observed in the data modeled to calculate Se(VI) binding constants to WPC (Fig. 3b). This may result in a high inherent error in that fit, manifested as higher V(Y) values for models that calculated WPC metal-sorbent binding constants (Table 3). Secondly, WPC may contribute carbon nanoparticles to solution, which are known to exist in woody biochar (Yan et al., 2014; Naghdi et al., 2017). Such nanoparticles may sorb Se (or Cd), pass through the 0.45 μm nylon membranes used to filter experimental supernatants, and then be mistakenly quantified as free metal in solution during ICP-MS/MS analysis. On a per-gram basis, WPC has a high capacity to sorb both Cd and Se (Fig. 2). Thirdly, it may be that components of the soils (e.g., clay, DOC) do interact substantially with the surface of WPC, and these artifacts only become measurable in the 5 g L^{-1} soil, 5 g L^{-1} WPC experiments. Finally, cation-induced anion adsorption might influence the degree of Se adsorption and thus the match of the adsorption experiment results with those of the predictive models (Bolan et al., 1999). As noted earlier (Zachara et al., 1992; Kulczycki et al., 2005; Alessi and Fein, 2010), interactions between sorbents and complexation of metals by solution ligands are two considerable

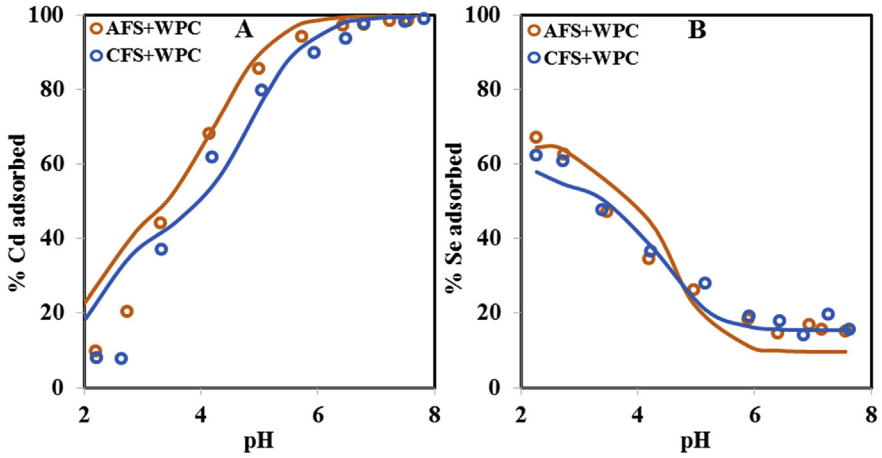

Fig. 4. Adsorption of (A) 100 μM Cd and (B) 100 μM Se, to mixtures of AFS (10 g L^{-1}) and WPC (1 g L^{-1}), and CFS (10 g L^{-1}) and WPC (1 g L^{-1}). Open symbols represent experimental data and solid lines represent model predictions of adsorption.

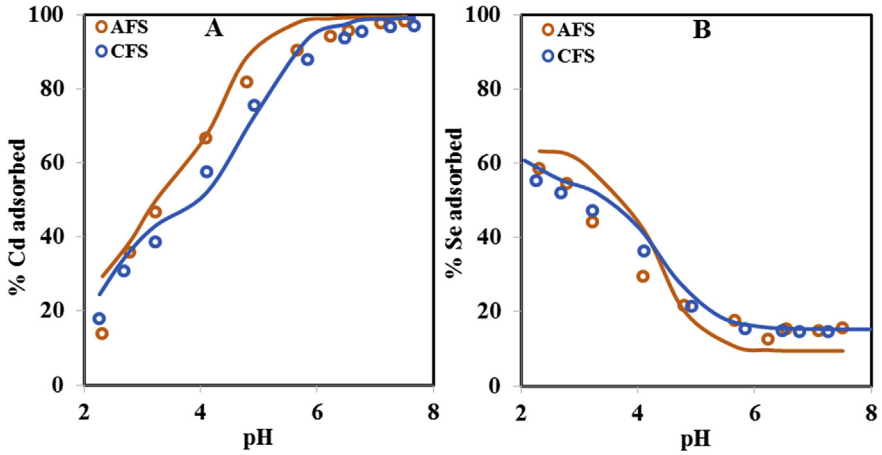

Fig. 5. Adsorption of a solution containing both 100 μM Cd and 100 μM Se to AFS (10 g L^{-1}) or CFS (10 g L^{-1}). Panel (A) shows Cd data, and (B) shows Se data. Open symbols represent experimental data and solid lines represent model predictions of adsorption.

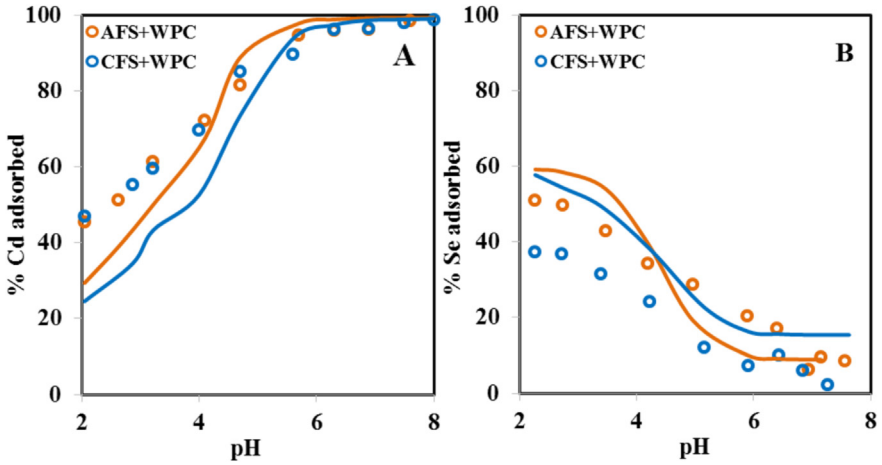

Fig. 6. Adsorption of a solution containing both 100 μM Cd and 100 μM Se adsorption to mixtures of either AFS (10 g L^{-1}) and WPC (1 g L^{-1}), or CFS (10 g L^{-1}) and WPC (1 g L^{-1}). Panel (A) shows Cd data, and (B) shows Se data. Open symbols represent experimental data and solid lines represent model predictions of adsorption.

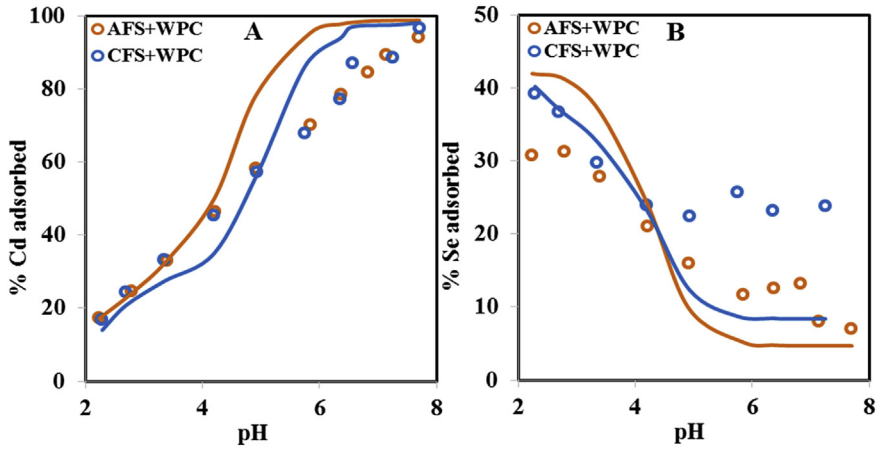

Fig. 7. Adsorption of a solution containing both 100 μM Cd and 100 μM Se adsorption to mixtures of either AFS (5 g L^{-1}) and WPC (5 g L^{-1}), or CFS (5 g L^{-1}) and WPC (5 g L^{-1}). Panel (A) shows Cd data, and (B) shows Se data. Open symbols represent experimental data and solid lines represent model predictions of adsorption.

limitations of the CA approach. However, it would be rare for soil to be amended with >10% (w/w) biochar (e.g., Novak et al., 2009; Van Zwieten et al., 2010; Igalavithana et al., 2017), and the predictions of our models in mixtures containing 10% or less biochar (w/w) match well to the experimental data.

4. Conclusions

The application of SCMs to predict the distribution of metals in biochar-amended soil systems has clear benefits because these models have the capability to account for the impacts of changes in pH, ionic strength, sorbent-to-sorbate ratio, and even temperature. The non-electrostatic surface complexation approach used here, the first ever SCM application to biochar-soil mixtures, was generally successful in predicting the equilibrium distribution of Cd and Se in mixtures containing those metals, biochar, and agricultural soil. However, several challenges remain. Above we note the presence of Se-DOC aqueous complexes, or Se and/or Cd bound to biochar-derived carbon nanoparticles, as potential explanations for the poor model predictions of experiments containing high concentrations of biochar. If the latter is true, nanoparticles could act as an additional vector of metals mobility in agricultural soils amended with biochar. Spectroscopic and microscopic investigations are needed to confirm the association of Cd and Se with nanoparticles and/or DOC in solution. Finally, to advance the application of surface complexation theory to soil-biochar systems, SCM studies on different types of biochar (e.g., pyrolysis temperature, feedstock) and biochar-soil mixtures are needed. The results of such studies can be combined with a robust extant literature of SCMs of soils and soil components, which can then be used to develop predictive models of numerous multi-component systems containing biochar as a sorbent.

Acknowledgements

This work was supported by NSERC Discovery Grants and an NSERC RTI award to DSA and KOK. LJR gratefully acknowledges support from a Vanier CGS.

Appendix A. Supplementary data

Supplementary data related to this article can be found at http://dx.doi.org/10.1016/j.apgeochem.2017.08.003.

References

Ahmad, M., Rajapaksha, A.U., Lim, J.E., Zhang, M., Bolan, N., Mohan, D., Vithanage, M., Lee, S.S., Ok, Y.S., 2014. Biochar as a sorbent for contaminant management in soil and water: a review. Chemosphere 99, 19–33.
Alam, M.S., Cossio, M., Robinson, L., Kenney, J.P.L., Wang, X., Konhauser, K.O., MacKenzie, M.D., Ok, Y.S., Alessi, D.S., 2016. Removal of organic acids from water using biochar and petroleum coke. Environ. Technol. Innov. 6, 141–151.
Alessi, D.S., Henderson, J.M., Fein, J.B., 2010. Experimental measurements of monovalent cation adsorption to Bacillus subtilis cells. Geomicrobiol. J. 27 (5), 464–472.
Alessi, D.S., Fein, J.B., 2010. Cadmium adsorption to mixtures of soil components: testing the component additivity approach. Chem. Geol. 270 (1–2), 186–195.
Anders, E., Watzinger, A., Rempt, F., Kitzler, B., Wimmer, B., Zehetner, F., Stahr, K., Zechmeister-Boltenstern, S., Soja, G., 2013. Biochar affects the structure rather than the total biomass of microbial communities in temperate soils. Agric. Food Sci. 22 (4), 404–423.
Anderson, G.M., 2005. Thermodynamics of Natural Systems, second ed. Cambridge University Press, Cambridge, United Kingdom, p. 664.
Andersson, A., Bingefors, S., 1985. Trends and annual variations in Cd concentrations in grain of winter wheat. Acta Agric. Scand. 35 (4), 339–344.
Banuelos, G., Schulin, R., Bitterli, C., 2013. Fate and movement of selenium from drainage sediments disposed onto soil with and without vegetation. Environ. Pollut. 180, 7–12.
Beesley, L., Moreno-Jimenez, E., Fellet, G., Carrijo, L., Sizmur, T., 2015. Biochar and heavy metals. In: Lehmann, J., Joseph, S. (Eds.), Biochar for Environmental Management: Science, Technology and Implementation, second ed. Earthscan, London, pp. 563–594.
Bethke, C.M., Brady, P.V., 2000. How the Kd approach undermines ground water cleanup. Ground Water 38 (3), 435–443.
Bolan, N.S., Naidu, R., Tillman, R.W., Khan, A., Syers, J.K., 1999. Effect of anion sorption on cadmium sorption by soils. Aust. J. Soil Res. 37, 445–460.
Bolan, N.S., Adriano, D.C., Mani, S., Khan, A.R., 2003. Adsorption, complexation and phytoavailability of copper as influenced by organic manure. Environ. Toxicol. Chem. 22, 450–456.
Bonten, L.T.C., Römkens, P.F.A.M., Brus, D.J., 2008. Contribution of heavy metal leaching from agricultural soils to surface water loads. Environ. Forensics 9, 252–257.
Cambardella, C.A., Moorman, T.B., Parkin, T.B., Karlen, D.L., Novak, J.M., Turco, R.F., Konopka, A.E., 1994. Field-scale variability of soil properties in central Iowa soils. Soil Sci. Soc. Am. J. 58 (5), 1501–1511.
Cox, J.S., Smith, D.S., Warren, L.A., Ferris, F.G., 1999. Characterizing heterogeneous bacterial surface functional groups using discrete affinity spectra for proton binding. Environ. Sci. Technol. 33, 4514–4521.
Davis, J.A., James, R.O., Leckie, J.O., 1978. Surface ionization and complexation at the oxide/water interface, I. Computation of electrical double layer properties in simple electrolytes. J. Colloid Interface Sci. 63 (3), 480–499.
Davis, J.A., 1984. Complexation of trace metals by adsorbed natural organic matter. Geochim. Cosmochim. Acta 48 (4), 679–691.
Davis, J.A., Coston, J.A., Kent, D.B., Fuller, C.C., 1998. Application of the surface complexation concept to complex mineral assemblages. Environ. Sci. Technol. 32, 2820–2828.
Dzombak, D.A., Morel, F.M.M., 1990. Surface Complexation Modeling: Hydrous Ferric Oxide. Wiley Interscience, New York, 393pp.
Fein, J.B., 2006. Thermodynamic modeling of metal adsorption onto bacterial cell walls: current challenges. Adv. Agron. 90, 179–202.
Fein, J.B., Daughney, C.J., Yee, N., Davis, T.A., 1997. A chemical equilibrium model for metal adsorption onto bacterial surfaces. Geochim. Cosmochim. Acta 61 (16),

3319–3328.
Flynn, S.L., Gao, Q., Robbins, L.J., Warchola, T., Weston, J.N.J., Alam, M.S., Liu, Y., Konhauser, K.O., Alessi, D.S., 2017. Measurements of bacterial mat metal binding capacity in alkaline and carbonate-rich systems. Chem. Geol. 451, 17–24.
Garrels, R.M., Christ, C.L., 1965. Solutions, Minerals, and Equilibria. Harper and Row, New York, p. 450.
Goldberg, S., 1992. Use of surface complexation models in soil chemical systems. Adv. Agron. 47, 233–329.
Goldberg, S., 2014. Modeling selenite adsorption behavior on oxides, clay minerals, and soils using the triple layer model. Soil Sci. 179 (12), 568–576.
Grant, C.A., Sheppard, S.C., 2008. Fertilizer impacts on cadmium availability in agricultural soils and crops. Hum. Ecol. Risk Assess. 14 (2), 210–228.
Herbelin, A.L., Westall, J.C., 1999. FITEQL: a Computer Program for Determination of Equilibrium Constants from Experimental Data. Department of Chemistry, Oregon State University, Corvallis, OR. Report 99–01.
Holmgren, G.G.S., Meyer, M.W., Chaney, R.L., Daniels, R.B., 1993. Cadmium, lead, zinc, copper, and nickel in agricultural soils of the United States of America. J. Environ. Qual. 22 (2), 335–348.
Igalavithana, A.D., Lee, S.-E., Lee, Y.H., Tsang, D.C.W., Rinklebe, J., Kwon, E.E., Ok, Y.S., 2017. Heavy metal immobilization and microbial community abundance by vegetable waste and pine cone biochar of agricultural soils. Chemosphere 174 (1), 593–603.
Kappler, A., Wuestner, M.L., Ruecker, A., Harter, J., Halama, M., Behrens, S., 2014. Biochar as an electron shuttle between bacteria and Fe(III) minerals. Environ. Sci. Technol. Lett. 1 (8), 339–344.
Kjeargsgaard, A.A., 1972. Reconnaissance Soil Survey of the Tawatinaw Map Sheet (83-I). Report No. S-72–39. Alberta Institute of Pedology, University of Alberta.
Komárek, M., Koretsky, C.M., Stephen, K.J., Alessi, D.S., Chrastný, V., 2015. Competitive adsorption of Cd(II), Cr(VI), and Pb(II) onto nanomaghemite: a spectroscopic and modeling approach. Environ. Sci. Technol. 49 (21), 12841–12859.
Koretsky, C., 2000. The significance of surface complexation reactions in hydrologic systems: a geochemist's perspective. J. Hydrol. 230, 127–171.
Kraepiel, A.M.L., Keller, K., Morel, F.M.M., 1999. A model for metal adsorption on montmorillonite. J. Colloid Interface Sci. 210, 43–54.
Kulczycki, E., Fowle, D.A., Fortin, D., Ferris, F.G., 2005. Sorption of cadmium and lead by bacteria-ferrihydrite composites. Geomicrobiol. J. 22 (6), 299–310.
Laird, D., Rogovska, N., 2015. Biochar effects on nutrient leaching. In: Lehmann, J., Joseph, S. (Eds.), Biochar for Environmental Management: Science, Technology and Implementation. Routledge, UK, pp. 521–542.
Lalonde, S., Konhauser, K.O., Amskold, L., McDermott, T., Inskeep, B.P., 2007a. Chemical reactivity of microbe and mineral surfaces in hydrous ferric oxide depositing hydrothermal springs. Geobiology 5, 219–234.
Lalonde, S., Amskold, L., Warren, L.A., Konhauser, K.O., 2007b. Surface chemical reactivity and metal adsorptive properties of natural cyanobacterial mats from an alkaline hot spring, Yellowstone National Park. Chem. Geol. 243, 36–52.
Lehmann, J., Kuzyakov, Y., Pan, G., Ok, Y.S., 2015. Biochars and the plant-soil interface. Plant Soil 395, 1–5.
Li, X., Coles, B.J., Ramsey, M.H., Thornton, I., 1995. Sequential extraction of soils for multielement analysis by ICP-AES. Chem. Geol. 124 (1–2), 109–123.
Liu, Y., Alessi, D.S., Owttrim, G.W., Petrash, D.A., MLoszewska, A.M., Lalonde, S.V., Martinez, R.E., Zhou, Q., Konhauser, K.O., 2015. Cell surface reactivity of Synechococcus sp. PCC 7002: implications for metal sorption from seawater. Geochim. Cosmochim. Acta 169, 30–44.
López-Granados, F., Jurado-Expósito, M., Atenciano, S., García-Ferrer, A., Sánchez de la Orden, M., García-Torres, L., 2002. Spatial variability of agricultural soil parameters in southern Spain. Plant Soil 246 (1), 97–105.
Lund, T.J., Koretsky, C.M., Landry, C.J., Schaller, M.S., Das, S., 2008. Surface complexation modeling of Cu(II) adsorption on mixtures of hydrous ferric oxide and kaolinite. Geochem. Trans. 9, 9.
Masiello, C.A., Chen, Y., Gao, X., Liu, S., Cheng, H.-Y., Bennett, M.R., Rudgers, J.A., Wagner, D.S., Zygourakis, K., Silberg, J.J., 2013. Biochar and microbial signaling: production conditions determine effects on microbial communication. Environ. Sci. Technol. 47 (20), 11496–11503.
Naghdi, M., Taheran, M., Pulicharla, R., Rouissi, T., Brar, S.K., Verma, M., Surampalli, R.Y., 2017. Pine-wood derived nanobiochar for removal of carbamazepine from aqueous media: adsorption behavior and influential parameters. Arab. J. Chem. http://dx.doi.org/10.1016/j.arabjc.2016.12.025.
Nambu, K., Yonebayashi, K., 1999. Acidic properties of dissolved organic matter leached from organic layers in temperate forests. Soil Sci. Plant Nutr. 45 (1), 65–77.
Novak, J.M., Busscher, W.J., Laird, D.L., Ahmedna, M., Watts, D.W., Niandou, M.A.S., 2009. Impact of biochar amendment on fertility of a Southeastern Coastal Plain soil. Soil Sci. 174 (2), 105–112.
Petrash, D.P., Raudsepp, M., Lalonde, S.V., Konhauser, K.O., 2011. Assessing the importance of matrix materials in biofilm chemical reactivity: insights from proton and cadmium adsorption onto the commercially-available biopolymer alginate. Geomicrobiol. J. 28 (3), 266–273.
Rees, F., Simonnot, M.O., Morel, J.L., 2014. Short-term effects of biochar on soil heavy metal mobility are controlled by intra-particle diffusion and soil pH increase. Euro. J. Soil Sci. 65, 149–161.
Robertson, G.P., Sollins, P., Ellis, B.G., Lajtha, K., 1999. Exchangeable ions, pH and cation exchange capacity. In: Robertson, G.P., Coleman, D.C., Bledsoe, C.S., Sollins, P. (Eds.), Standard Soil Methods for Long-term Ecological Research. LTER, New York, NY, USA.
Römkens, P.F.A.M., Plette, A.C.C., Verstappen, G.G.C., 2002. Contribution of agriculture to the heavy metal loads of Dutch surface waters. In: Steenvoorden, J.H.A.M., Claessen, F., Willems, J. (Eds.), Agricultural Effects on Ground and Surface Waters: Research on the Edge of Science and Society, vol. 273. IAHS, Walligford, UK, publ., pp. 337–342
Schroth, B.K., Sposito, G., 1997. Surface charge properties of clays. Clays Clay Miner. 45, 85–91.
Smith, D.S., Kramer, J.R., 1999. Multi-site proton interactions with natural organic matter. Environ. Int. 25 (2–3), 307–314.
Tan, J., Zhu, W., Wang, W., Li, R., Hou, S., Wang, D., Yang, L., 2002. Selenium in soil and endemic diseases in China. Sci. Total Environ. 284 (1–3), 227–235.
Tessier, A., Campbell, P.G., Bisson, M., 1979. Sequential extraction procedure for the speciation of particulate trace metals. Anal. Chem. 51 (7), 844–851.
Uchimiya, M., Lima, I.M., Klasson, K.T., Wartelle, L.H., 2010. Contaminant immobilization and nutrient release by biochar soil amendment: roles of natural organic matter. Chemosphere 80, 935–940.
Verheijen, F.G.A., Graber, E.R., Ameloot, N., Bastos, A.C., Sohi, S., Knicker, H., 2014. Biochars in soils: new insights and emerging research needs. Eur. J. Soil Sci. 65 (1), 22–27.
Van Zwieten, L., Kimber, S., Morris, S., Chan, K.Y., Downie, A., Rust, J., Joseph, S., Cowie, A., 2010. Effects of biochar from slow pyrolysis of papermill waste on agronomic performance and soil fertility. Plant Soil 327 (1), 235–246.
Vithanage, M., Rajapaksha, A.U., Ahmad, M., Uchimiya, M., Dou, X., Alessi, D.S., Ok, Y.S., 2015. Mechanisms of antimony adsorption onto soybean stover-derived biochar in aqueous solution. J. Environ. Manage 151, 443–449.
von Gunten, K., Alam, M.S., Hubmann, M., Ok, Y.S., Konhauser, K.O., Alessi, D.S., 2017. Modified sequential extraction for biochar and petroleum coke: metal release potential and its environmental implications. Bioresour. Technol. 236, 106–110.
Westall, J.C., 1982. FITEQL, a Computer Program for Determination of Chemical Equilibrium Constants from Experimental Data, Version 2.0. Department of Chemistry, Oregon State University, Corvallis, OR. Report 82–02.
Woolf, D., Amonette, J.E., Street-Perrott, F.A., Lehmann, J., Joseph, S., 2010. Sustainable biochar to mitigate global climate change. Nat. Commun. 1 art. no 56.
Yan, Y., Toghiani, H., Cai, Z., Zhang, J., 2014. Formation of nanocarbon spheres by thermal treatment of woody char from fast pyrolysis process. Wood Fiber Sci. 464 (4), 437–450.
Zachara, J.M., Smith, S.C., Resch, C.T., Cowan, C.E., 1992. Cadmium sorption to soil separates containing layer silicates and iron and aluminum oxides. Soil Sci. Soc. Am. J. 56, 1074–1084.
Zhang, Q.-Z., Dijkstra, F.A., Liu, X.-R., Wang, Y.-D., Huang, J., Lu, N., 2014. Effects of biochar on soil microbial biomass after four years of consecutive application in the North China plain. PLoS One 9 (7), e102062.
Zhang, Y., Luo, W., 2014. Adsorptive removal of heavy metal from acidic wastewater with biochar produced from anaerobically digested residues: kinetics and surface complexation modeling. BioResources 9 (2), 2484–2499.
Zhao, J., Dong, Y., Xie, X., Li, X., Zhang, X., Shen, X., 2011. Effect of annual variation on available soil nutrients in pear orchards. Acta Ecol. Sin. 31 (4), 212–216.